# Arbitrary Pulse Width in the Four-Pulse NMR Experiment

MICHAEL MEHRING

Institut für Physik der Universität Dortmund, Germany

(Z. Naturforsch. **27 a**, 1634—1639 [1972]; received 16 September 1972)

Coherent averaging during rf irradiation can be utilized in the four-pulse nmr experiment in order to cancel the average dipolar interaction in solids. Thus an arbitrary pulse width can be used in the four-pulse experiment, leading to a total rotation angle $\beta_1 \geqq 90^\circ$ of the rf pulses depending on the duty factor. Ideal timing is achieved in the classical Waugh, Huber, Häberlen sequence.

## 1. Introduction

The classical four-pulse experiment as invented by WAUGH, HUBER, and HÄBERLEN [1, 2] has been proven to be very effective in reducing the dipolar broadening in the nmr spectra of solids and unravelling weaker interactions such as magnetic shielding anisotropies, $J$-coupling etc. [3]. There is a considerable amount of other types of line narrowing experiments which are capable of reducing dipolar broadening, but they will not be dealt with here [4].

In the classical four-pulse experiment the rf pulses were considered as $\delta$ pulses, i. e. pulse width $t_{\text{p}} = 0$. By applying a cycle of rf pulses to the spins, the interaction Hamiltonian becomes modulated, i. e. time dependent. If this modulated interaction Hamiltonian is now averaged over a cycle, it can be made to vanish for certain types of interaction (f. e. dipolar and quadrupolar) and on the other hand retained, but scaled by a scalingfactor $S$ (e. g. magnetic shielding $S < 1$, $J$-coupling $S = 1$), for others [2].

Thus far it has been assumed, that the rf pulses in the four-pulse experiment had to be $\delta$ pulses in order to achieve line narrowing and only small deviations from zero pulse width could be compensated for by making the total rotation angle $\beta_1 > 90^\circ$ [2]. It will be demonstrated, however, in Sect. 2 that coherent averaging takes place also during rf irradiation.

This can be utilized, as shown in Sect. 3, to operate the four-pulse experiment with any finite pulse width up to an upper limit, given by the timing of the four-pulse sequence. The total rotation angle $\beta_1$ of the rf pulses has to be increased gradually with increasing pulse width up to the limit of $\beta_{\text{u}} = 116^\circ\ 14'$ for the upper pulse width limit [5]. Operating the four-pulse experiment with long rf pulses has some advantages over the common procedure of making the pulses as short as possible. Since the rf power needed is proportional to $H_1^2$ a considerable reduction in rf power is obtained in going to longer pulse widths, thus avoiding all the problems involved with high power transmitters, probe arcing and heating, receiver blocking etc.

The last section treats the effect of finite pulse width on the dipolar echo formation by using the modified four-pulse sequence.

Reprint requests to Prof. Dr. M. MEHRING, Institut für Physik der Universität Dortmund, *D-4600 Dortmund-Eichlinghofen*, Baroper Straße.

## 2. Coherent Averaging during RF Irradiation

If we call the Hamiltonian describing the coupling of the spins due to internal interaction $\mathcal{H}_{\text{int}}$ and the Hamiltonian which describes the coupling of the spins to external fields $\mathcal{H}_{\text{ext}}$, we can express the total Hamiltonian as

$$\mathcal{H} = \mathcal{H}_{\text{int}} + \mathcal{H}_{\text{ext}}\,. \tag{1}$$

Let us follow the treatment of Ref. [2] where the propagator $L(t)$ which governs the time dependence of the spin density matrix has been expressed by the product

$$L(t) = L_1(t) \cdot L_2(t) \tag{2}$$

where $L_1(t)$ contains only $\mathcal{H}_{\text{ext}}$ and $L_2(t)$ contains the modulated interaction Hamiltonian $\widetilde{\mathcal{H}}(t)$, namely

$$L_1(t) = T \cdot \exp\left\{ -i \int_0^t \mathrm{d}t'\, \mathcal{H}_{\text{ext}}(t') \right\}, \tag{3 a}$$

$$L_2(t) = T \cdot \exp\left\{ -i \int_0^t \mathrm{d}t'\, \widetilde{\mathcal{H}}(t') \right\}, \tag{3 b}$$

$$\widetilde{\mathcal{H}}(t) = L\,(t)\, \mathcal{H}_{\text{int}}\, L_1(t) \tag{3 c}$$

where $T$ is the Dyson time ordering operator.

With an rf field applied in the $x$- or $y$-direction of the rotating frame respectively, the "external" Hamiltonian can be written as

$$\mathcal{H}_{\text{ext}} = -\omega_1(t)\, I_{x,y} \tag{4}$$

with $\omega_1(t) = \gamma H_1(t)$.

Leading to the propagator

$$L_1(t) = e^{i\beta(t)\, I_{x,y}}$$

with

$$\beta(t) = \int_0^t \mathrm{d}t'\, \omega_1(t'). \tag{5}$$

Since $L_1(t)$ operates only on the spin dependent part of the interaction Hamiltonian in Eq. (3 c), $\mathcal{H}_{\text{int}}$ is conveniently written as a product of tensor operators [6, 7]

$$\mathcal{H}_{\text{int}} = \sum_{M=-j}^{+j} (-1)^M A_{j,-M}\, T_{jM} \tag{6}$$

where the different interactions can be distinguished by $j$ ($j=1$ magnetic shielding, $j=2$ dipolar and quadrupolar interaction).

The spin dependent part $T_{jM}$ is modulated according to Eqs. (3 c), (5) and leads in the rotating frame to

$$\tilde{\mathcal{H}}(t) \propto \tilde{T}_{j0} \tag{7}$$

where [6]

$$\tilde{T}_{j0} = [L_1^{-1}(t)\, T_{jM}\, L_1(t)]_{M=0} \tag{8}$$

which can be expressed as

$$\tilde{T}_{j0} = \sum_{M=-j}^{+j} T_{jM}\, D^{(j)}_{M0}(\alpha, \beta, 0), \tag{9}$$

where the Wigner matrices [7] $D^{(j)}_{M0}$ can be written as

$$D^{(j)}_{M0}(\alpha, \beta, 0) = e^{-iM\alpha}\, d^{(j)}_{M0}(\beta) \tag{10}$$

and where $\alpha$ determines the rf field direction.

Using Eqs. (9), (10) we obtain:

(i) $y$-irradiation ($\alpha = 0$)

$$\tilde{T}_{10} = T_{10} \cos\beta + (T_{1-1} - T_{1+1}) \frac{1}{\sqrt{2}} \sin\beta, \tag{11 a}$$

$$\begin{aligned} T_{20} = T_{20}\, &\tfrac{1}{2}(3\cos^2\beta - 1) \\ &+ (T_{2-1} - T_{2+1}) \sqrt{\tfrac{3}{2}} \sin\beta \cos\beta \\ &+ (T_{2+2} + T_{2-2}) \sqrt{\tfrac{3}{8}} \sin^2\beta, \end{aligned} \tag{11 b}$$

(ii) $x$-irradiation ($\alpha = -\pi/2$).

The terms with $M = \pm 1$ in Eq. (11) are multiplied by $\pm i$, whereas the terms with $M = \pm 2$ are multiplied by $-1$. The average Hamiltonian during rf irradiation is immediately obtained as

$$\overline{T}_{j0}(\beta_1) = \frac{1}{\beta_1} \int_0^{\beta_1} \mathrm{d}\beta\, \tilde{T}_{j0} \tag{12}$$

where $\beta_1 = \int_0^{t_p} \mathrm{d}t\, \omega_1(t)$.

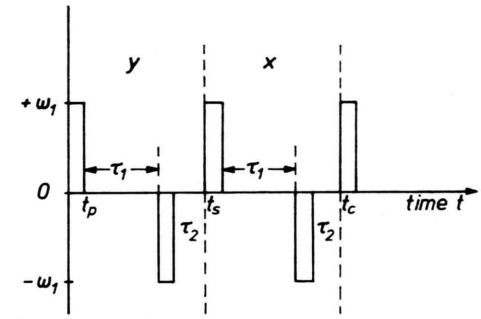


Fig. 1. Timing of the four-pulse sequence, where $t_p$ is the pulse width, and with the cycle times $t_s$ of the subcycle and $t_c$ of the full cycle. There are two "windows" of duration $\tau_1$ and $\tau_2$ in each subcycle. $y$ and $x$ denote the direction of rf irradiation in the rotating frame.

The way in which the average Hamiltonian over a cycle of rf pulses can be calculated will be demonstrated in the case of the subcycle of the four-pulse experiment (see Fig. 1), which is essentially a phase alternated pulse experiment with cycle time

$$t_s = 2\, t_p + \tau_1 + \tau_2\,.$$

If we use the abbreviation $k = \tau_1/\tau_2$ and introduce the duty factor $\delta = 2\, t_p/t_s$ we obtain the average Hamiltonian over the cycle time $t_s$ as

$$\langle \tilde{T}_{j0} \rangle_{\text{ts}} = \delta \overline{T}_{j0}(\beta_1) + \frac{k(1-\delta)}{1+k} \tilde{T}_{j0}(\beta_1) + \frac{(1-\delta)}{1+k} \tilde{T}_{j0}(0) \tag{13}$$

which can be written in compact form as

$$\langle \tilde{T}_{j0} \rangle_{\text{ts}} = \sum_{M=-j}^{+j} T_{jM}\, \overline{D^{(j)}_{M0}(\alpha, \beta, 0)} \tag{14}$$

where the coefficients $\overline{D^{(j)}_{M0}(\alpha, \beta, 0)}$ can be derived by using Eqs. (9) – (13). By using the abbreviation

$$\begin{aligned} D_0 &= \overline{D^{(2)}_{00}(0, \beta, 0)}, \\ D_1 &= -\overline{D^{(2)}_{10}(0, \beta, 0)} = \overline{D^{(2)}_{-10}(0, \beta, 0)}, \\ D_2 &= \overline{D^{(2)}_{20}(0, \beta, 0)} = \overline{D^{(2)}_{-20}(0, \beta, 0)}, \\ C_0 &= \overline{D^{(1)}_{00}(0, \beta, 0)}, \\ C_1 &= -\overline{D^{(1)}_{10}(0, \beta, 0)} = \overline{D^{(1)}_{-10}(0, \beta, 0)}, \end{aligned} \tag{15}$$

we obtain from Eqs. (9) – (15):

$$D_0 = \tfrac{3}{2}\cos\beta_1\left[\frac{k(1-\delta)}{1+k}\cos\beta_1 + \delta\,\frac{\sin\beta_1}{2\,\beta_1}\right] + \frac{1+(1-k)}{2\cdot(1+k)}\,(1-(3/2)\,\delta)\,, \tag{16 a}$$

$$D_1 = \sqrt{\tfrac{3}{8}}\sin\beta_1\left[\delta\,\frac{\sin\beta_1}{\beta_1} + \frac{2\,k(1-\delta)}{1+k}\cos\beta_1\right], \tag{16 b}$$

$$D_2 = \sqrt{\tfrac{3}{8}}\left[\sin\beta_1\left(\frac{k(1-\delta)}{1+k}\cdot\sin\beta_1 - \frac{\delta}{2\,\beta_1}\cos\beta_1\right) + \delta/2\right] \tag{16 c}$$

$$C_0 = \delta\,\frac{\sin\beta_1}{\beta_1} + \frac{k(1-\delta)}{1+k}\cos\beta_1 + \frac{(1-\delta)}{(1+k)}\,, \tag{16 d}$$

$$C_1 = \frac{\delta}{\sqrt{2}\,\beta_1}\,(1-\cos\beta_1) + \frac{1}{\sqrt{2}}\,\frac{k(1-\delta)}{1+k}\cdot\sin\beta_1\,. \tag{16 e}$$

The coefficients corresponding to irradiation in $x$-direction ($\alpha = -90^\circ$) are easily obtainend by multiplying $D^{(j)}_{M0}(0,\beta,0)$ by $\pm i$ in the case of $M=\pm 1$ and by $-1$ in the case of $M=\pm 2$.

Thus scaling of second rank tensor interaction (e.g. dipolar interaction) and first rank tensor interaction (e.g. magnetic shielding) in phase alternated pulsed nmr experiments can be easily calculated by combining Eqs. (14), (15), (16). From Eq. (16 c) it follows that $D_2$ never can be made to vanish, besides trivial cases like $\beta_1 = 0$, i.e. the dipole interaction cannot be cancelled in a phase alternated experiment, where rf irradiation takes place only in one direction in the rotating frame. However, if another subcycle is added in which irradiation is performed orthogonal to the first one, $D_2$ is multiplied by $-1$ in the second subcycle and the total average vanishes, independent of the parameters $\delta$, $k$ and $\beta_1$.

## 3. The Four-Pulse Experiment with Arbitrary Pulse Width

The timing of the four-pulse cycle with arbitrary pulse width is shown in Figure 1. The full cycle with the cycle time $t_c$ consists of two subcycles with the cycle time $t_s$ each, in which rf irradiation is performed in the $y$- and $x$-direction respectively.

The average Hamiltonian can be expressed as

$$\langle \widetilde{T}_{j0}\rangle_{t_c} = \tfrac{1}{2}\,\langle \widetilde{T}_{j0}\rangle^{(y)}_{t_s} + \tfrac{1}{2}\,\langle \widetilde{T}_{j0}\rangle^{(x)}_{t_s} \tag{17}$$

Since the term with $M=\pm 2$ in $\langle \widetilde{T}_{j0}\rangle_{t_c}$ vanishes independent of $\delta$, $k$ and $\beta_1$ due to phase quadrature as mentioned above, the condition for line narrowing can be expressed as

$$\langle \widetilde{T}_{20}\rangle_{t_c} = 0; \quad \text{i.e.} \quad D_0 = D_1 = 0 \tag{18}$$

whereas $\langle \widetilde{T}_{10}\rangle_{t_c} \neq 0$.

Thus we arrive at the question, for which set of $(\delta, k, \beta_1)$ do $D_0$ and $D_1$ simultaneously vanish. From Eqs. (16 a, b) it can be shown, that this condition can be fulfilled only if

$$\delta = \frac{2}{3}\,\frac{k-2}{k-1}\,. \tag{19}$$

This puts a restriction on the timing of the four-pulse sequence and it demands what we shall call the "ideal timing". This "ideal timing" is nothing else, but the timing of the classical four-pulse cycle [1] in the $\delta$ pulse approximation i.e. $k=2$ if $\delta=0$. If the pulse width is increased, the leading edge of the pulse is kept at the location of the $\delta$ pulse in the cycle, and the pulse width is simply increased to the right, as shown in Figure 1. Under this condition the duty factor obeys Equation (19).

If the condition Eq. (19) is inserted in Eq. (16) we can write

$$D_0 = \tfrac{3}{2}\cos\beta_1\left(\tfrac{1}{3}\,(2-\tfrac{3}{2}\,\delta)\cos\beta_1 + \frac{\sin\beta_1}{2\,\beta_1}\right), \tag{20 a}$$

$$D_1 = \sqrt{\tfrac{3}{8}}\sin\beta_1\left[\frac{\sin\beta_1}{\beta_1} + \tfrac{2}{3}\,(2-\tfrac{3}{2}\,\delta)\cos\beta_1\right], \tag{20 b}$$

$$D_2 = \sqrt{\tfrac{3}{8}}\left[\sin\beta_1\left(\tfrac{1}{3}\,(2-\tfrac{3}{2}\,\delta)\sin\beta_1 - \frac{\delta}{2\,\beta_1}\cos\beta_1\right) + \delta/2\right], \tag{20 c}$$

$$C_0 = \delta\,\frac{\sin\beta_1}{\beta_1} + \tfrac{1}{3}\,(2-\tfrac{3}{2}\,\delta)\cos\beta_1 + \tfrac{3}{2}\,(1-\tfrac{3}{2}\,\delta)\,, \tag{20 d}$$

$$C_1 = \frac{1}{\sqrt{2}}\left[\frac{\delta}{\beta_1}\,(1-\cos\beta_1) + \tfrac{1}{3}\,(2-\tfrac{3}{2}\,\delta)\sin\beta_1\right] \tag{20 e}$$

which yields the scaling factors in the case of the "ideal timing".

$D_0$ and $D_1$ are plotted versus $\beta_1$ in Fig. 2 for different values of $\delta$. It is interesting to compare this with far off-resonance effects [8]. It can be seen, that $D_0$ and $D_1$ cross the zero line for the same value of $\beta_1$ as is demanded by the "line narrowing" condition Equation (18).

This condition ($D_0 = D_1 = 0$) leads to a dependence of the rotating angle $\beta_1$ on the duty factor $\delta$

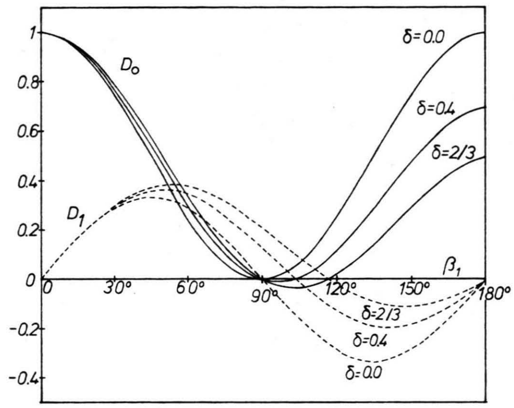


Fig. 2. The remaining coefficients $D_0$ and $D_1$ in the average dipolar Hamiltonian in the four-pulse experiment with "ideal timing" according to Eq. (20 a, b) are plotted versus $\beta_1$ for different values of the duty factor $\delta$. — Due to the "ideal timing" $D_0$ and $D_1$ cross the zero line always at the same value $\beta_1$.

accordinig to Eq. (20 a) and (20 b) as follows:

$$\delta = \tfrac{4}{3}/(1-\tan\beta_1/\beta_1)\ . \qquad (21)$$

$\delta$ is plotted versus $\beta_1$ according to Eq. (21) in Figure 3. This figure can serve as a diagram for determining $\beta_1$ for a given value of $\delta$, i. e. there is for any given $\delta$ with $0 \leqq \delta \leqq 2/3$ a value $\beta_1$ for which line narrowing in solids can be achieved. For

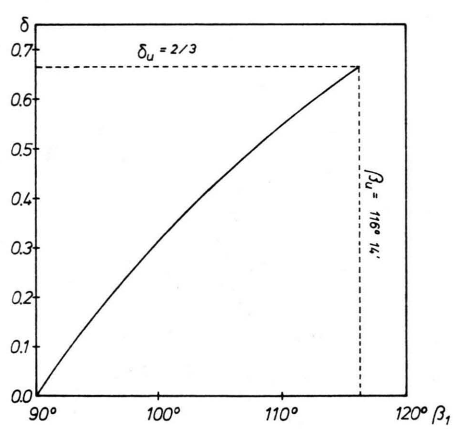


Fig. 3. The duty factor $\delta$ versus $\beta_1$ is plotted according to Eq. (21) up to the limit $\delta_u=2/3$; $\beta_u=116°\ 14'$ (see text). A monotonic increase of $\beta_1$ with $\delta$ is observed, so that for any given $\delta$ there is only one $\beta_1$ for which line narrowing in solids can be obtained.

a small duty factor $\delta$, $\beta_1$ may be expressed as $\beta_1 = \pi/2 + \varepsilon$ where $\varepsilon$ is small. In this case Eq. (21) leads to

$$\delta = \tfrac{2}{3}\,\pi \cdot \varepsilon$$

which is the same result as Eq. (67) of Ref. [2].

The following procedure for adjusting the four-pulse experiment is suggested:

(i) set up the "ideal timing" according to Figure 1,
(ii) adjust the proper phases,
(iii) increase or decrease the rf power (not the pulse width!) in order to obtain a lengthened decay.

One must not change the pulse width, since in general this does not fulfill Equation (21).

There is an upper limit for $\delta$, which is given by the timing according to Equation (19). This upper limit is reached if $k=\infty$ $\delta_u = 2/3$ leading to the condition [5] [see Eq. (21)]

$$\tan\beta_u = -\beta_u \qquad (22)$$

from which follows

$$\beta_u = 116°\ 14'.$$

The capability of achieving line narrowing in solids with such a four-pulse experiment in the ultimate pulse width limit is described elsewhere [5].

The scaling factor $S$ of the magnetic shielding in a four-pulse experiment and all other interactions which can be described by a first rank tensor operator can be expressed as

$$S = (C_0{}^2 + C_1{}^2)^{1/2} \qquad (23)$$

where $C_0$ and $C_1$ are given by Eqs. (20 d, e) under the condition of Equation (21).

An analytical expression for $S$ as a function of $\beta_1$ can be obtained from Eqs. (20 d, e), (21), but is of not much interest here. Since the duty factor $\delta$ is an easily measurable quantity, we have calculated numerically $S$ as a function of $\delta$ by using Eq. (20 d, e) and Equation (21). $S$ is plotted versus $\delta$ in Figure 4.

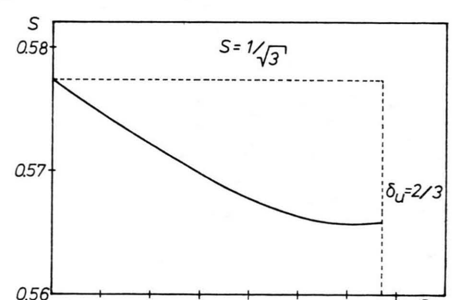


Fig. 4. The scaling factor $S$ for magnetic shielding in the four-pulse experiment is plotted versus the duty factor $\delta$ according to Eqs. (20 d, e), (21), (23), up to the upper pulse width limit $\delta_u$.

The scaling factor $S$ for the magnetic shielding begins with $S=1/\sqrt{3}=0{,}577$ for $\delta=0$ and decreases with increasing $\delta$, until the upper limit in pulse width is reached ($\delta_u=2/3$), corresponding to $S=0.565$. Nevertheless, the variation of the scaling factor $S$ with $\delta$ is seen to be very small.

The first order and all other higher correction Hamiltonians of odd order can be shown to vanish due to symmetry arguments [6, 9].

## 4. The Dipolar Echo produced by the Four-Pulse Sequence

A dipolar echo can be produced, using the four-pulse sequence [10, 11], utilizing the fact that the average dipolar Hamiltonian can be made negative [10, 11] if the parameter $k$ becomes greater than 2.

In the case of $\delta$ pulses, this can be shown easily by using the parameters $\delta=0$ and $\beta_1=90°$ in Equation (16). It follows from Eqs. (16 a, b) that under these conditions [10, 11]

$$D_0=\frac{1}{2}\cdot\frac{2-k}{1+k} \tag{24}$$

whereas

$$D_1=0 .$$

Thus the average dipolar Hamiltonian becomes negative for $k>2$ during a burst of four-pulse cycles of duration $t_B$. The motion of the spins governed by this negative average Hamiltonian redevellopes in time when the subsequent positive Hamiltonian $T_{20}$ is in effect. The echo condition can be written as

$$\frac{1}{2}\,\frac{2-k}{1+k}\cdot t_B+t-t_B=0$$

or

$$t/t_B=\tfrac{3}{2}\,k/(1+k) \tag{25}$$

leading to the formation of an echo at time $t$, when the four-pulse burst is terminated at time $t_B$ [10].

If a finite pulse width ($\delta\neq0$) is used, the problem of forming a dipolar echo is more complicated, but can be solved by the means of Equation (16). $D_1$ can be made to vanish according to Eq. (16 b) if

$$\delta=1\Big/\Big(1-\frac{1+k}{2\,k\,\beta_1}\tan\beta_1\Big). \tag{26}$$

In Fig. 5 the duty factor $\delta$ is plotted versus $\beta_1$ for different parameters $k$, according to Equation (26).

If $\delta$ according to Eq. (26) is inserted in Eq. (16 a) we obtain

$$D_0=\frac{1+\tan\beta_1(k-2)/k\,\beta_1}{4-2\tan\beta_1(1+k)/k\,\beta_1}. \tag{27}$$

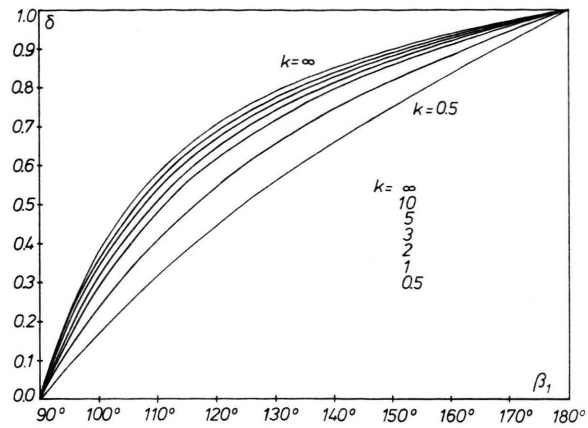


Fig. 5. The duty factor $\delta$ according to Eq. (26) for different values of $k$ is plotted versus the rotating angle $\beta_1$. This diagram serves in choosing the parameter sets ($\delta$, $k$, $\beta_1$) for obtaining a dipolar echo.

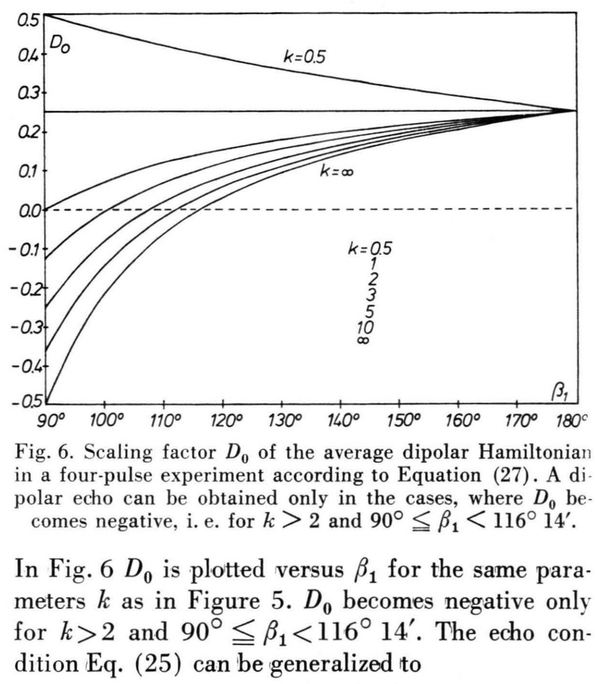


Fig. 6. Scaling factor $D_0$ of the average dipolar Hamiltonian in a four-pulse experiment according to Equation (27). A dipolar echo can be obtained only in the cases, where $D_0$ becomes negative, i. e. for $k>2$ and $90°\leqq\beta_1<116°\,14'$.

In Fig. 6 $D_0$ is plotted versus $\beta_1$ for the same parameters $k$ as in Figure 5. $D_0$ becomes negative only for $k>2$ and $90°\leqq\beta_1<116°\,14'$. The echo condition Eq. (25) can be generalized to

$$D_0\,t_B+t-t_B=0$$

leading to

$$t/t_B=1-D_0 \tag{28}$$

where $D_0$ is given by Eq. (27) with the parameters $k$ and $\beta_1$ obtained by Equation (26). From Eqs. (26) and (27) it follows, that for any duty factor $\delta$ with $0\leqq\delta<2/3$ a dipolar echo can be obtained.

*Acknowledgment*

Valuable discussion and conversation with Professors O. Kanert and J. S. Waugh is greatfully acknowledged.

[1] J. S. WAUGH, L. M. HUBER, and U. HÄBERLEN, Phys. Rev. Letters **20**, 180 [1968].
[2] U. HÄBERLEN and J. S. WAUGH, Phys. Rev. **175**, 453 [1968].
[3] J. D. ELLETT, U. HÄBERLEN, and J. S. WAUGH, Polymer Letters **7**, 71 [1969]. — M. MEHRING, R. G. GRIFFIN, and J. S. WAUGH, J. Chem. Phys. **55**, 746 [1971]; J. Amer. Chem. Soc. **92**, 7222 [1970]. — L. M. STACEY, R. W. VAUGHAN, and D. D. ELLEMAN, Phys. Rev. Letters **26**, 1153 [1971]. — R. G. GRIFFIN et al., J. Chem. Phys. (in press) [1972].
[4] P. MANSFIELD, Pulsed NMR in Solids, Progress in Nuclear Magnetic Resonance Spectroscopy, edited by J. W. EMSLEY, J. FEENEY, and L. H. SUTCLIFF, Vol. 8, part 1, p. 41, 1971, and references therein.
[5] M. MEHRING, Rev. Sci. Instrum. **44** [1973].
[6] M. MEHRING and J. S. WAUGH, Phys. Rev. **5 B**, 3459 [1972].
[7] D. M. BRINK and G. R. SATCHLER, Angular Momentum, Clarendon Press, p. 22, Oxford University Press 1968.
[8] U. HÄBERLEN, J. D. ELLETT, and J. S. WAUGH, J. Chem. Phys. **55**, 53 [1971]. — A. PINES and J. S. WAUGH, to be published.
[9] P. MANSFIELD, J. Phys. C **4**, 1444 [1971].
[10] A. PINES, W.-K. RHIM, and J. S. WAUGH, J. Mag. Res. **6**, 457 [1972].
[11] H. SCHNEIDER and H. SCHMIEDEL, Phys. Lett. **30 A**, 298 [1969]. — W.-K. RHIM, A. PINES, and J. S. WAUGH, Phys. Rev. Lett. **25**, 218 [1970]; Phys. Rev. **3 B**, 684 [1971].


# Transporteigenschaften von $Bi_{70}Sb_{30}$

G. SCHNEIDER und R. TRINKS

Institut für Technische Physik der Technischen Universität Braunschweig

(Z. Naturforsch. **27 a**, 1639—1645 [1972]; eingegangen am 12. August 1972)

*Transport Properties of $Bi_{70}Sb_{30}$*

Crystals of the composition $Bi_{70}Sb_{30}$, undoped and doped with the donor Te and the acceptor Sn, were made by zone melting. Specimens were prepared with the long edges parallel to the bisectrix, the binary or the trigonal axis. Transport properties (electrical resistance, transverse magnetoresistance, Hall effect, thermoelectric power, longitudinal and transverse Nernst-Ettingshausen effect) were measured for specimens with different orientation and doping in the temperature range from 8 to 300 °K. Investigations of magnetic field dependence of some properties and of the anisotropy of magnetoresistance in a transverse field of different directions were made.

## 1. Einleitung

Bi-Sb-Legierungen erweisen sich im Konzentrationsgebiet von etwa 5 bis 40 At.-% Sb als Halbleiter mit kleiner Energielücke, in den übrigen Konzentrationsbereichen liegt Überlappung der Bänder vor [1, 2]. Diese Legierungen wie ihre Komponenten erscheinen einmal interessant bezüglich der Anisotropie ihrer Eigenschaften [3], zum anderen sind sie wegen der hohen Ladungsträgerbeweglichkeiten gut geeignet für Untersuchungen unter den Bedingungen von hohen Magnetfeldern [4]. Bisher wurden besonders Bi-reiche Legierungen mit Sb-Konzentrationen bis zu 12 – 15 At.-Proz. Sb (Maximum der Energielücke) untersucht [2, 5–8], darüber hinaus liegen verhältnismäßig wenige Ergebnisse vor [2, 9–11]. Das liegt wohl u. a. daran, daß die Energiebandstruktur mit zunehmendem Sb-Gehalt immer mehr von der schon ziemlich gut bekannten des reinen Bi abweicht und zudem eine gute Einkristallherstellung immer schwieriger wird. In der hier vorliegenden Arbeit wurden nun die elektrischen Transportgrößen von $Bi_{70}Sb_{30}$ untersucht, und zwar undotiert sowie mit Te- bzw. Sn-Dotierung.

## 2. Probenherstellung und Meßverfahren

Als Ausgangsmaterialien dienten Wismut und Antimon mit einer Reinheit von 99,9999% (Koch & Light, Colnbrook). Die Legierungen wurden in evakuierten, abgeschmolzenen Quarzampullen über einige Stunden bei 720 °C zusammengeschmolzen. Zur Einkristallherstellung erfolgte dann Zonenschmelzen dieses Materials in einem Quarzrohrofen, wobei die Rohrheizung 220 °C und die Zonenheizung 450 °C einstellten. Der Zonenheizer wurde von einem mechanisch weitgehend vom Quarzrohrofen getrennten Motor mit zugehöriger Führung mit einer Geschwindigkeit von 0,8 bzw. 1,6 mm/h bewegt. Bei der größeren Geschwindigkeit wuchsen die Kristalle bevorzugt mit der senkrecht zur trigonalen Achse liegenden Ebene parallel zur Ziehrichtung. Aus

Tab. 1.

| Proben-Nr. | Zusammensetzung | Orientierung |
|---|---|---|
| 1 | $Bi_{70}Sb_{30}$ | Bisektrix ‖ Probenachse |
| 2 | $Bi_{70}Sb_{30}$+0,1 At.-Proz. Te | Bisektrix ‖ Probenachse |
| 3 | $Bi_{70}Sb_{30}$+0,1 At.-Proz. Sn | Bisektrix ‖ Probenachse |
| 4 | $Bi_{70}Sb_{30}$ | bin. Achse ‖ Probenachse |
| 5 | $Bi_{70}Sb_{30}$+0,1 At.-Proz. Te | bin. Achse ‖ Probenachse |
| 6 | $Bi_{70}Sb_{30}$ | trig. Achse ‖ Probenachse |